# Rotational Isomerization Barriers of Thiophene Oligomers in the Ground and First Excited Electronic States. A $^1$H NMR and Fluorescence Lifetime Investigation

**J. C. Horne, G. J. Blanchard,* and E. LeGoff**

*Contribution from the Department of Chemistry and Center for Fundamental Materials Research, Michigan State University, East Lansing, Michigan 48824-1322*

*Received April 24, 1995*[⊗]

**Abstract:** We report on the isomerization dynamics of a family of substituted thiophene oligomers designed for the synthesis of soluble poly(alkylthiophene)s possessing a minimal coupling defect density. The data we report for 3′,4′-dibutyl-2,2′:5′,2″-terthiophene, 3″,4″-dibutyl-2,2′:5′,2″:5″,2‴:5‴,2⁗-pentathiophene, and 3′,4′,3⁗,4⁗-tetrabutyl-2,2′:5′,2″:5″,2‴:5‴,2⁗:5⁗,2⁗′:5⁗′,2⁗′′-sexithiophene indicate that the ground state isomerization barrier for all of these oligomers is on the order of 8 kcal/mol, with no discernible dependence on the length of the oligomer. For oligomer isomerization in the $S_1$ electronic state, we find that the isomerization barrier for both the pentathiophene and sexithiophene oligomer is ~5.2 kcal/mol, slightly larger than the value we reported previously for $S_1$ 3′,4′-dibutyl-2,2′:5′,2″-terthiophene. Experimental data for both electronic states in these oligomers are in excellent agreement with semiempirical calculations using the PM3 parametrization.

## Introduction

Determining the intrinsic, structural limits to the synthesis of conjugated polymers possessing a minimum defect density is a central issue in the development of practical organic optical and electronic devices. Understanding and controlling the extent of structural disorder in a material is also critical to studies aimed at optimizing the nonlinear optical response of strongly coupled three-level systems.[1,2] There are a limited number of conjugated polymers for which it is possible to synthesize crystalline materials possessing a very low structural defect density. For the majority of conjugated polymer systems, however, syntheses are by electrochemical or, less commonly, photochemical means and are often carried out in solution. For this reason, any amount of structural heterogeneity intrinsic to the monomer units will be expressed in the resulting polymer. We focus here on poly(alkylthiophene) because of the importance of this family of materials for conducting[3−8] and nonlinear optical information processing[9−13] applications.

Polythiophenes and poly(alkylthiophene)s have received a great deal of recent attention for both fundamental and practical reasons. This family of polymers has found application in the fabrication of organic light-emitting diodes, and for this reason, there has been a significant amount of research effort aimed at producing processable materials with a minimal density of structural defects. The first polythiophenes were synthesized from thiophene and the dominant defect in this material was from inter-ring linkages between positions α and β to the S heteroatom on adjacent thiophene rings.[14] These materials are also insoluble and, as a result, were of limited utility for device applications requiring material processability. The next advance in the synthesis of polythiophenes was to use a 3-alkylthiophene as the monomer.[15−20] While the solubility of the resulting polymer was improved, head-to-head and tail-to-tail coupling defects contributed significantly to molecular scale disorder in the resultant material. There have been several successful attempts to minimize these coupling defects synthetically by using asymmetric monomers, and it is now possible to make poly(3-alkylthiophene)s where the inter-ring coupling is ~95% "pure", *i.e.* head-to-tail coupling.[6,21−23] An alternative approach to such syntheses is to use oligomeric forms of thiophenes where head-to-tail coupling defects are precluded for structural reasons. Recent work by Wang *et al.*[5] has shown this to be a successful approach, yielding corresponding polymer material that exhibits

* Author to whom correspondence should be addressed.

[⊗] Abstract published in *Advance ACS Abstracts,* August 15, 1995.

(1) Hambir, S. A.; Blanchard, G. J.; Baker, G. L. *J. Chem. Phys.* **1995**, *102*, 2295.
(2) Hambir, S. A.; Wolfe, D.; Blanchard, G. J.; Baker, G. L. In preparation.
(3) Wang, C.; Benz, M. E.; LeGoff, E.; Schindler, J. L.; Allbritton-Thomas, J.; Kannewurf, C. R.; Kanatzidis, M. G. *Chem. Mater.* **1994**, *6*, 401.
(4) DeWitt, L.; Blanchard, G. J.; LeGoff, E.; Benz, M. E.; Liao, J.-H.; Kanatzidis, M. G. *J. Am. Chem. Soc.* **1993**, *115*, 12158.
(5) Wang, C.; Benz, M. E.; LeGoff, E.; Schindler, J. L.; Kannewurf, C. R.; Kanatzidis, M. G. *Polym. Prepr.* **1993**, *34*, 422.
(6) McCullough, R. D.; Lowe, R. D. *J. Chem. Soc., Chem. Commun.* **1992**, *70*.
(7) Guay, J.; Kasai, P.; Diaz, A.; Wu, R.; Tour, J. M.; Dao, L. H. *Chem. Mater.* **1992**, *4*, 1097.
(8) Roncali, J. *Chem. Rev.* **1992**, *92*, 711.
(9) Nunzi, J.-M.; Pfeffer, N.; Charra, F. *Chem. Phys. Lett.* **1993**, *215*, 114.
(10) Robitaille, L.; Leclerc, M.; Callender, C. L. *Chem. Mater.* **1993**, *5*, 1755.
(11) Beljonne, D.; Shuai, Z.; Bredas, J. L. *J. Chem. Phys.* **1993**, *98*, 8819.
(12) Thienpont, H.; Rikken, G. L. J. A.; Meijer, E. W.; ten Hoeve, W.; Wynberg, H. *Phys. Rev. Lett.* **1990**, *65*, 2141.
(13) Zhao, M.-T.; Singh, B. P.; Prasad, P. N. *J. Chem. Phys.* **1988**, *89*, 5535.
(14) Gamaggi, G. M.; Deluca, G.; Tundo, A. *J. Chem. Soc., Perkin Trans. 2* **1972**, 1594.
(15) Jen, K. Y.; Miller, G. G.; Elsenbaumer, R. L. *J. Chem. Soc., Chem. Commun.* **1986**, 1346.
(16) Sato, M.; Tanaka, S.; Kaeriyama, K. *J. Chem. Soc., Chem. Commun.* **1986**, 873.
(17) Hotta, S.; Rughooputh, S. D. D. V.; Heeger, A. J.; Wudl, F. *Macromolecules* **1987**, *20*, 212.
(18) Nowak, M.; Rughooputh, S. D. D. V.; Hotta, S.; Heeger, A. J. *Macromolecules* **1987**, *20*, 965.
(19) Rughooputh, S. D. D. V.; Nowak, M.; Hotta, S.; Heeger, A. J.; Wudl, F. *Synth. Met.* **1987**, *21*, 41.
(20) Rugooputh, S. D. D. V.; Hotta, S.; Heeger, A. J.; Wudl, F. *J. Polym. Sci., Polym. Phys.* **1987**, *25*, 1071.
(21) McCullough, R. D.; Tristam-Nagle, S.; Williams, S. P.; Lowe, R. D.; Jayaraman, M. *J. Am. Chem. Soc.* **1993**, *115*, 4910.
(22) Tour, J. M.; Wu, R. *Macromolecules* **1992**, *25*, 1901.
(23) Benz, M. E. Ph.D. Thesis, Michigan State University, East Lansing, MI, 1992.

0002-7863/95/1517-9551$09.00/0 

conductivities higher than those reported for poly(thiophene)s synthesized from 3-alkylthiophene monomers. Even with the development of synthetic routes aimed at minimizing the extent of inter-ring coupling defects, rotational isomerization between individual thiophene rings in oligomeric and polymeric thiophenes can give rise to a different class of structural defects. For this reason it is important to consider the intrinsic inter-ring isomerization characteristics of thiophene oligomers, and to understand how the energetics of isomerization in this family of oligomers are affected by oligomer length. We have examined the rotational isomerization characteristics of three substituted thiophene oligomers in order to address these questions. In a previous report[4] we had indicated that the ground state isomerization barrier of 3′,4′-dibutyl-2,2′:5′,2″-terthiophene (DBTT) was ~20 kcal/mol based on variable-temperature $^1$H NMR measurements. Further investigation of this system with a higher field (500 MHz) NMR spectrometer has revealed that the data reported previously were limited in resolution, causing our estimate of the isomerization barrier to be too large. The data we report here possess the resolution required to establish the ground state isomerization barrier of DBTT, and two larger oligomers, to be ~8 kcal/mol. Measurements of the excited state isomerization characteristics of thiophene oligomers indicate this energy to be ~5.2 kcal/mol for both the substituted pentathiophene and sexithiophene compounds. We had found in our earlier report that the isomerization energy for the substituted terthiophene oligomer is 4.2 ± 0.4 kcal/mol.[4] We discuss below the means used to acquire the experimental data, the form and temperature dependence of the $^1$H NMR data and the way in which we relate the NMR chemical shift results to the dynamical response of the molecule, and the viscosity dependence of the fluorescence lifetime data for the pentathiophene and sexithiophene oligomers. In addition, we present semiempirical calculations[24-28] for these molecules using the PM3 parametrization. The PM3 parametrization offers a significant improvement over the AM1 parametrization for these oligomers. The calculated predictions are in excellent agreement with experimental data.

## Experimental Section

**Chemicals.** The thiophene oligomer 3′,4′-dibutyl-2,2′:5′,2″-terthiophene (DBTT) was synthesized according to a published procedure.[23] To synthesize the 3″,4″-dibutyl-2,2′:5′,2″:5″,2‴:5‴,2⁗-pentathiophene oligomer (DBPtT), DBTT was dibrominated at the α positions of the terminal thiophene rings using tetramethylammonium tribromide and subsequently coupled on both ends to thiophene magnesium bromide in the presence of a catalyst. The 3′,4′,3⁗,4⁗-tetrabutyl-2,2′:5′,2″:5″,2‴:5‴,2⁗:5⁗,2⁗′:5⁗′,2⁗″-sexithiophene oligomer (TBSxT) was synthesized by coupling 2 equiv of DBTT which had been treated sequentially with *n*-butyllithium and copper chloride. A detailed description of these oligothiophenes has been reported elsewhere.[29] For the fluorescence lifetime measurements, all solvents were purchased from the Aldrich Chemical Co. as either reagent grade or spectroscopic grade and were used without further purification. For the $^1$H NMR measurements, $d_8$-toluene (99.6 atom% D) was purchased from Isotech, Inc. and used as received.

**Steady State Optical Spectroscopy.** The absorption spectra of DBPtT and TBSxT were measured using a Hitachi U-4001 UV−visible spectrophotometer. The emission spectra for these oligomers were determined using a Hitachi F-4500 fluorescence spectrophotometer.

**Table 1.** Excitation and Emission Wavelengths Used for TCSPC Measurements

| | DBPtT | | TBSxT | |
|---|---|---|---|---|
| solvent | $\lambda_{exc}$ (nm) | $\lambda_{em}$ (10 nm bandwidth) | $\lambda_{exc}$ (nm) | $\lambda_{em}$ (10 nm bandwidth) |
| methanol | 390 | 481 | 406 | 504 |
| 1-butanol | 390 | 484 | 406 | 507 |
| 1-heptanol | 390 | 485 | 406 | 508 |
| 1-decanol | 390 | 485 | 406 | 508 |

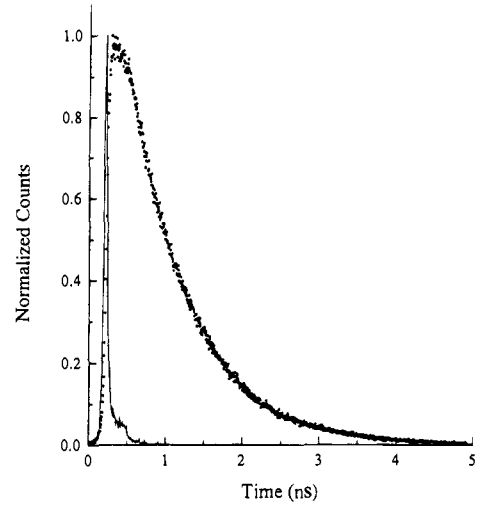


**Figure 1.** Example of excited state population decay for TBSxT in *n*-butanol. The instrumental response time is ~40 ps fwhm.

These data were used to determine the appropriate excitation and observation wavelengths for the fluorescence lifetime measurements.

**NMR Spectroscopy.** $^1$H NMR spectra of DBTT, DBPtT, and TBSxT in $d_8$-toluene, referenced to tetramethylsilane (TMS), were measured using a 500 MHz Varian (VXR-500) NMR spectrometer. The temperature of the samples was controlled with an FTS Systems air-jet and temperature control unit and was varied between −40 and +90 °C for DBPtT and TBSxT measurements and between −40 and +105 °C for DBTT measurements. Uncertainty in the sample temperature was determined to be 0.5 °C.

**Time Correlated Single Photon Counting Spectroscopy.** The spectrometer we used for the fluorescence lifetime measurements of the oligomers DBPtT and TBSxT has been described in detail before,[4,30] and we provide only a brief review of its salient characteristics here. The light pulses used to excite the sample are generated with a cavity-dumped, synchronously pumped dye laser (Coherent 702-2) excited by the second harmonic of the output of a mode-locked CW Nd:YAG laser (Quantronix 416). DBPtT was excited at 390 nm (LDS 751, Exciton, $LiIO_3$ Type I SHG), and TBSxT was excited at 405 nm (LDS 821, Exciton, $LiIO_3$ Type I SHG). Fluorescence was collected at 54.7° with respect to the polarization of the excitation pulse at the wavelengths indicated in Table 1. A representative fluorescence lifetime scan, together with the instrumental response function (typically ~40 ps fwhm), is shown in Figure 1.

**Data Analysis.** The lifetimes we report here are derived from data deconvoluted from the instrumental response function using software written by Snyder and Demas.[31] The lifetimes we report are averages and standard deviations of at least 12 individual determinations for each solvent.

**Calculations.** Semiempirical calculations[24-28] were performed using Hyperchem Release 4.0 on an IBM compatible PC (Gateway 2000 486-66V). The PM3 parametrization, used for these calculations, is a modification of the AM1 parametrization that treats molecules containing polar heteroatoms, such as sulfur, more accurately than previous parametrizations. The calculation strategy for the three oligomers was to perform an initial optimization of the structures using a molecular

(24) Dewar, M. J. S.; Zoebisch, E. G.; Healy, E. F.; Stewart, J. J. P. *J. Am. Chem. Soc.* **1985**, *107*, 3902.
(25) Dewar, M. J. S.; Dieter, K. M. *J. Am. Chem. Soc.* **1986**, *108*, 8075.
(26) Stewart, J. J. P. *Comput.-Aided Mol. Des.* **1990**, *4*, 1.
(27) Dewar, M. J. S.; Thiel, W. *J. Am. Chem. Soc.* **1977**, *99*, 4899.
(28) Dewar, M. J. S.; Thiel, W. *J. Am. Chem. Soc.* **1977**, *99*, 4907.
(29) Liao, J.-H.; Benz, M. E.; LeGoff, E.; Kanatzidis, M. G. *Adv. Mater.* **1994**, *6*, 135.
(30) Holtom, G. R. *Proc. SPIE* **1990**, *1402*, 2.
(31) Snyder, S.; Demas, J. N. Private communication.

**Chart 1.** Structures and Interring Rotations for the Three Thiophene Oligomers: (a) 3′,4′-Dibutyl-2,2′:5′,2″-terthiophene (DBTT), (b) 3″,4″-Dibutyl-2,2′:5′,2″:5″,2‴:5‴,2⁗-pentathiophene (DBPtT), and (c) 3′,4′,3⁗,4⁗-Tetrabutyl-2,2′:5′,2″:5″

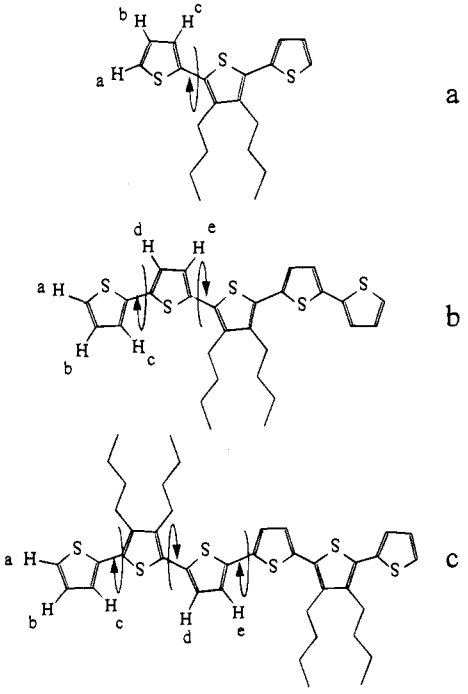


mechanics routine (MM+)[32] followed by a geometry optimization at the semiempirical level using an SCF algorithm. Semiempirical optimization was performed until the lowest energy conformation for each molecule was attained. Heats of formation and electronic charges of individual protons and carbons were calculated for the geometrically optimized molecules.

## Results and Discussion

The primary focus of this paper is to obtain information on the isomerization characteristics of the thiophene oligomers DBTT, DBPtT, and TBSxT (Chart 1), in both their ground and first excited singlet electronic states. The motivation for this work is to understand the intrinsic limits to conformational disorder in polymers synthesized from these oligomers and, based on this information, determine whether there is a preferred synthetic strategy for alkylated thiophene polymers. Because the measurement strategy for the isomerization of a molecule in its ground state differs significantly from that for excited state measurements, we will treat measurements of rotational isomerization in these two states separately.

**Ground State Measurements.** Representative $^1$H NMR spectra are shown for each of the three oligomers in Figures 2−4. The proton assignments are as indicated in Chart 1. The chemical shift of each proton exhibits a unique temperature dependence, from 0.0001 to 0.002 ppm/K, as shown for a series of DBTT spectra in Figure 5. Analogous protons on different oligomers exhibit almost identical temperature dependencies. Measurements of proton resonances that appear furthest downfield were limited, due to the presence of solvent peaks in the same chemical shift range. In a previous examination of DBTT, we had observed, using a 300 MHz NMR spectrometer, that the several doublet resonances split by ~1.5 Hz appeared to coalesce and, based on this information, we reported an isomerization barrier of ~20 kcal/mol for ground state DBTT.[4] Our subsequent measurements using a higher field spectrometer have shown that the apparent coalescence we reported earlier is actually only a loss of resolution. The split resonances for a given individual proton do not coalesce, because the splittings arise from *J*-coupling between non-adjacent protons. On the basis of the higher resolution data we report here for DBTT, DBPtT, and TBSxT, we conclude that ring rotation is much

(32) Allinger, N. L. *J. Am. Chem. Soc.* **1977**, *99*, 8127.

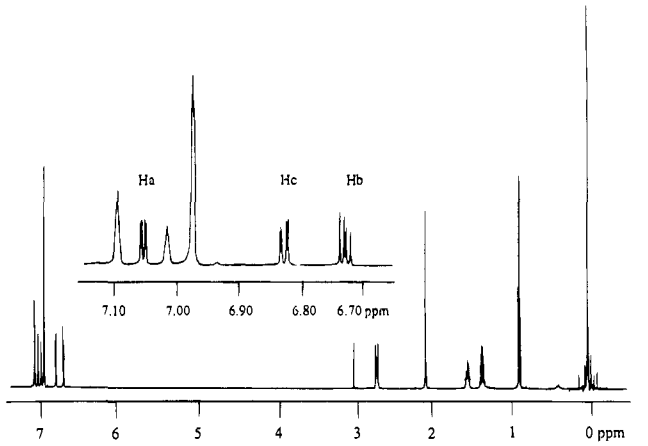


**Figure 2.** $^1$H NMR spectrum of DBTT taken at −20 °C. Inset: Expanded aromatic proton region with proton assignments for the aromatic protons. The designations of the protons are indicated in Chart 1.

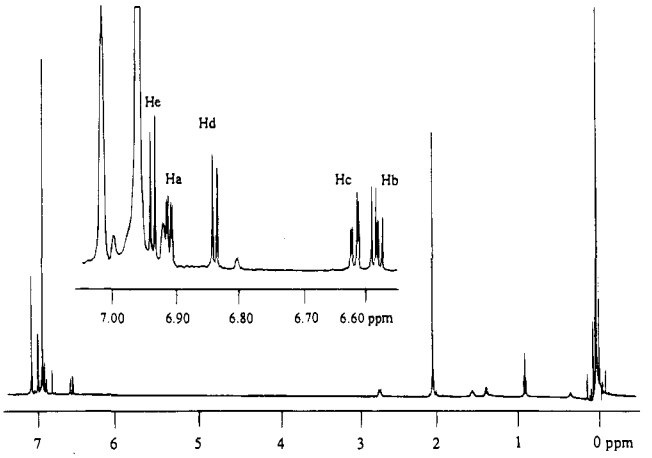


**Figure 3.** $^1$H NMR spectrum of DBPtT taken at −20 °C. Inset: Expanded aromatic proton region with proton assignments for the aromatic protons. The designations of the protons are indicated in Chart 1.

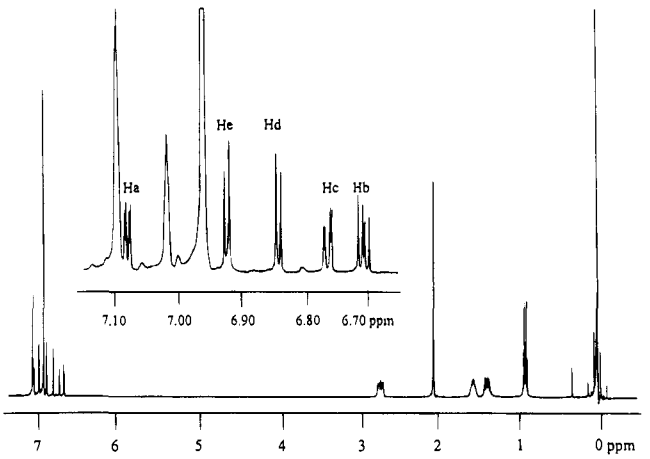


**Figure 4.** $^1$H NMR spectrum of TBSxT taken at −20 °C. Inset: Expanded aromatic proton region with proton assignments for the aromatic protons. The designations of the protons are indicated in Chart 1.

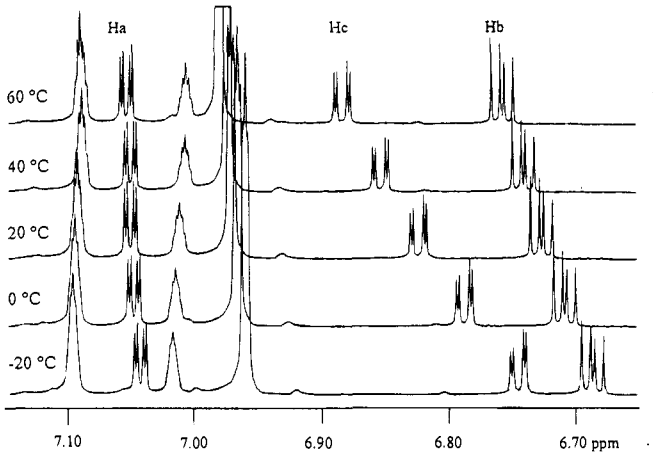


**Figure 5.** Temperature dependence of the aromatic proton resonances of DBTT, shown at five representative temperatures, as indicated.

faster than the time scale of the NMR experiment. That is, coalescence occurs at a temperature much lower than −40 °C for these oligomers. The rotational isomerization barriers for these oligomers are, in fact, significantly smaller than 20 kcal/mol. Despite the absence of a coalescence in these data, the temperature dependence of the proton chemical shifts for these oligomers can be used to infer the approximate energy of the isomerization barrier. We understand the temperature dependence of the individual proton resonances in these oligomers based on the temperature-dependent conformational distribution of the rotamers.

It is well-established that the chemical shift of a proton bound to an aromatic system is related to the effective charge on the carbon atom to which the proton is bound.[33-35]

$$\Delta\delta_H = a\Delta q_C \qquad (1)$$

The effective charge ($q_C$) on the carbon of interest is determined by its electron density, and the $^1$H NMR resonance energies (chemical shifts, $\delta$) are also affected by secondary, inductive effects such as "ring current".[35-37] We expect the effective charge on the proton to play a central role in determining the chemical shift, although we are not aware of any explicit treatments of the relationship between proton charge and chemical shift. We find, in fact, that the proton charges play a critical role in determining the proton NMR resonance frequency, and the carbon $\pi$ electron density is important as well (*vide infra*). The proportionality constant $a$ can be determined for a given system,[33,38] but it is not expected to be constant for all molecules because of secondary, structure-dependent shielding effects. We understand and model the temperature-dependent proton resonance energies for the thiophene oligomers as follows. The charge of each proton is influenced by the interring dihedral angle between individual thiophene rings. Because there is a finite energy barrier to interring rotation (Figures 6a, 7a, and 8a), the extent to which each rotamer will contribute depends on the temperature of the system. We have calculated the conformation dependence of the proton and adjacent carbon charge (Figures 6b,c, 7b,c, and 8b,c) as well as the isomerization barrier for inter-ring rotation (Figures 6a, 7a, and 8a) for each oligomer using semiempirical molecular orbital calculations with the PM3 parametrization. We calculated the charge for each aromatic proton and carbon at 5-deg increments between 0 and 180 °C. We assume in our treatment that there are no anomalies on this energy surface that would give rise to discontinuities (*e.g.* sudden polarization phenomena[39-42]). The *average* charge of a given proton or a given carbon for an oligomer isomerizing in solution, then, depends on the amount of time that the oligomer exists in each rotational conformation. This treatment presumes that ring rotation is fast compared to the time scale of the NMR

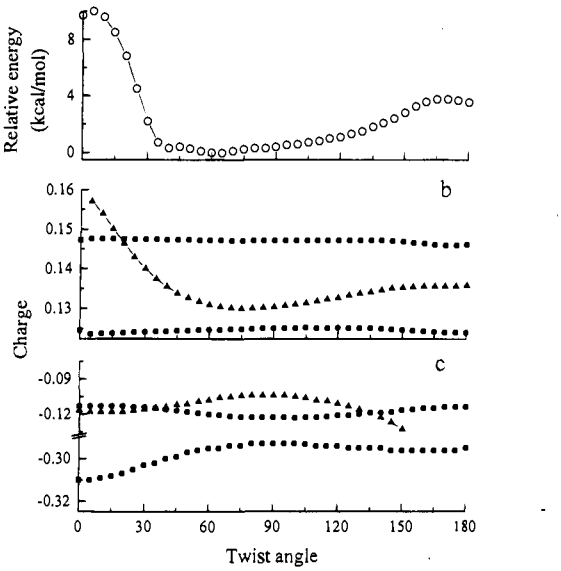


**Figure 6.** (a) Calculated isomerization barrier for DBTT, where the isomerization coordinate is taken as the interring dihedral angle. (b) Dependence of the proton charges on interring rotation angle: (■) $H_a$, (●) $H_b$, (▲) $H_c$. (c) Dependence of the aromatic carbon charges on interring rotation angle: (■) $C_a$, (●) $C_b$, (▲) $C_c$.

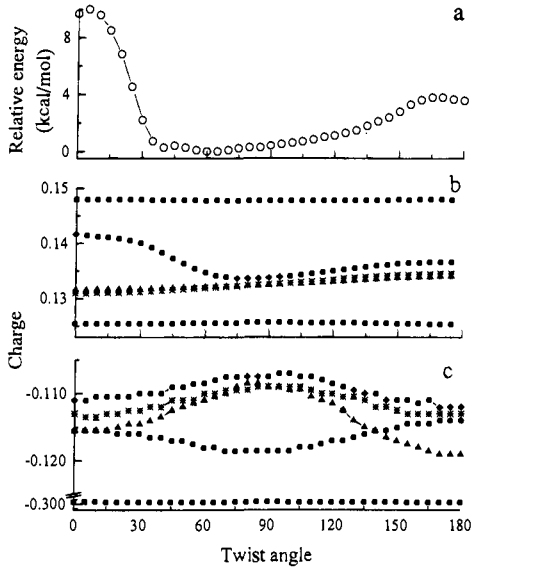


**Figure 7.** (a) Calculated isomerization barrier for DBPtT, where the isomerization coordinate is taken as the interring dihedral angle. (b) Dependence of the proton charges on interring rotation angle: (■) $H_a$, (●) $H_b$, (▲) $H_c$, (*) $H_d$, (♦) $H_e$. (c) Dependence of the aromatic carbon charges on interring rotation angle: (■) $C_a$, (●) $C_b$, (▲) $C_c$, (*) $C_d$, (♦) $C_e$.

(33) Fraenkel, G.; Carter, R. E.; McLachlan, A.; Richards, J. H. *J. Am. Chem. Soc.* **1960**, *82*, 5846.
(34) Cobb, T. B.; Memory, J. D. *J. Chem. Phys.* **1969**, *50*, 4262.
(35) Memory, J. D.; Wilson, N. K. *NMR of Aromatic Compounds*; John Wiley and Sons: New York, 1982.
(36) Pauling, L. *J. Chem. Phys.* **1936**, *4*, 673.
(37) Bernstein, H. J.; Schneider, W. G.; Pople, J. A. *Proc. R. Soc.* **1956**, *A236*, 515.
(38) Musher, J. I. *J. Chem. Phys.* **1962**, *37*, 34.
(39) Bonacic-Koutecky, V. *J. Am. Chem. Soc.* **1978**, *100*, 396.
(40) Salem, L. *Acc. Chem. Res.* **1979**, *12*, 87.
(41) Malrieu, J. P. *Theor. Chim. Acta* **1981**, *59*, 251.
(42) Lam, B.; Johnson, R. P. *J. Am. Chem. Soc.* **1983**, *105*, 7479.

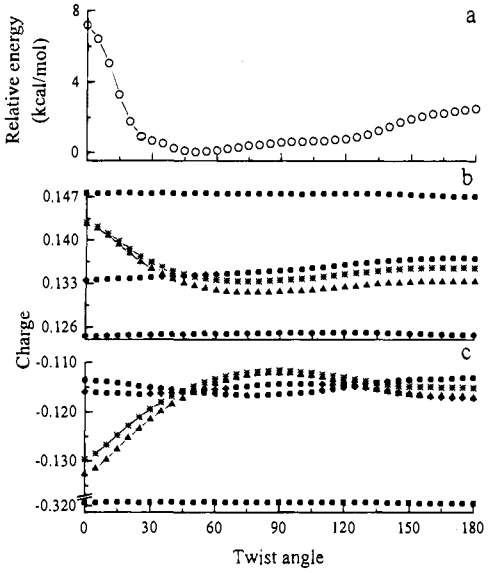


**Figure 8.** (a) Calculated isomerization barrier for TBsxT, where the isomerization coordinate is taken as the interring dihedral angle. (b) Dependence of the proton charges on interring rotation angle: (■) $H_a$, (●) $H_b$, (▲) $H_c$, (*) $H_d$, (♦) $H_e$. (c) Dependence of the aromatic carbon charges on interring rotation angle: (■) $C_a$, (●) $C_b$, (▲) $C_c$, (*) $C_d$, (♦) $C_e$.

measurement and that we sample a thermally-weighted portion of the isomerization surface. Changes in temperature thus alter the contribution of high energy portions of the isomerization surface to the average charges sampled in the NMR measurements. To determine the fractional contribution of a given conformer to the average charge of a given proton or carbon, the energy of the oligomer was calculated as a function of interring dihedral angle. For DBTT, there is one unique isomerization to consider. For DBPtT there are two distinct dihedral angles relevant to the isomerization surface, and for TBSxT there are three relevant dihedral angles, as shown in Chart 1. In this treatment of DBPtT and TBSxT we assume that the individual isomerization coordinates are nominally uncoupled (this is a valid assumption because the barriers are small), and thus the average of the two isomerization barriers provides a useful one-dimensional potential well representation for these molecular motions on the time scale of the NMR measurement. This assumption allows us to calculate ring rotation-dependent atomic charges without accounting for inductive, multiple-ring effects. From these energy surfaces, reduced to one-dimensional representations of the overall molecular motion, we can determine the contribution (fractional population) of a given rotamer based on the Boltzmann distribution because the isomerization is driven thermally.

$$N_\theta/N_0 = \exp(-(E_\theta - E_0)/k_B T) \qquad (2)$$

where $N_\theta$ is the population of the rotamer with diheral angle $\theta$, $N_0$ is the population of the lowest energy conformation, and the energies $E_\theta$ and $E_0$ are the relative energies of the two conformers.

We assume that the degeneracy of each conformer is the same, and include no degeneracy weighting factors in eq 2. For each atom of interest, the average charge density at a given temperature $T$, $\bar{q}_T$, weighted for the appropriate rotamer distribution, can be calculated from

$$\bar{q}_T = (\sum_\theta N_\theta q_\theta / \sum_\theta N_\theta)_T \qquad (3)$$

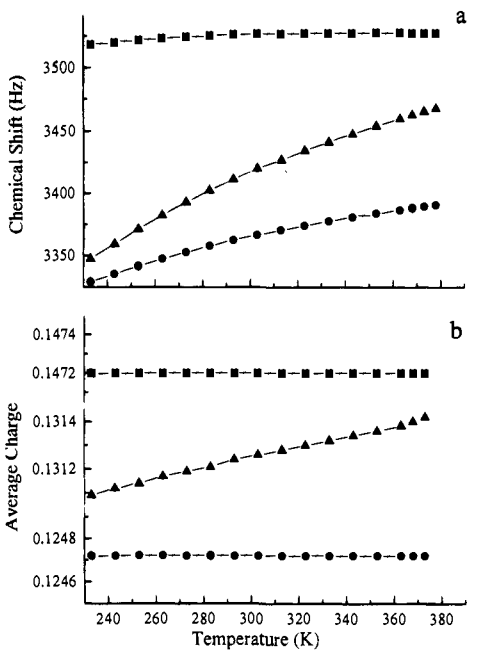


**Figure 9.** (a) Experimental temperature dependence of $^1$H NMR resonances for DBTT. (b) Temperature dependence of aromatic proton charges, calculated as described in the text. For both a and b: (■) $H_a$, (●) $H_b$, (▲) $H_c$.

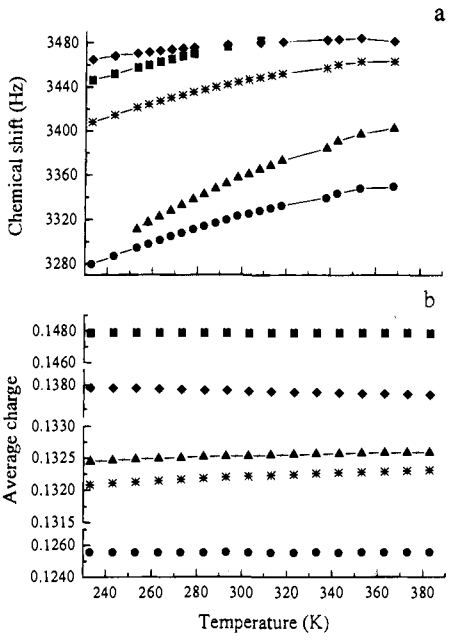


**Figure 10.** (a) Experimental temperature dependence of $^1$H NMR resonances for DBPtT. (b) Temperature dependence of aromatic proton charges, calculated as described in the text. For both a and b: (■) $H_a$, (●) $H_b$, (▲) $H_c$, (*) $H_d$, (♦) $H_e$.

The temperature dependence of $\bar{q}_T$ results from the Boltzmann terms. We obtain $\bar{q}_T$ for each relevant proton and carbon in these oligomers accordingly. A plot of the experimental temperature dependencies of the aromatic proton resonances for DBTT is shown in Figure 9a and a corresponding plot of $\bar{q}_T$ vs $T$ for these same protons is shown in Figure 9b. We present the same comparison for DBPtT and TBSxT in Figures 10 and 11, respectively. The temperature dependence of the average charge on a given proton correlates well with the experimental chemical shift temperature dependence. We note that the poorest agreement between experiment and calculation is for DBPtT, where the approximation of an average isomerization

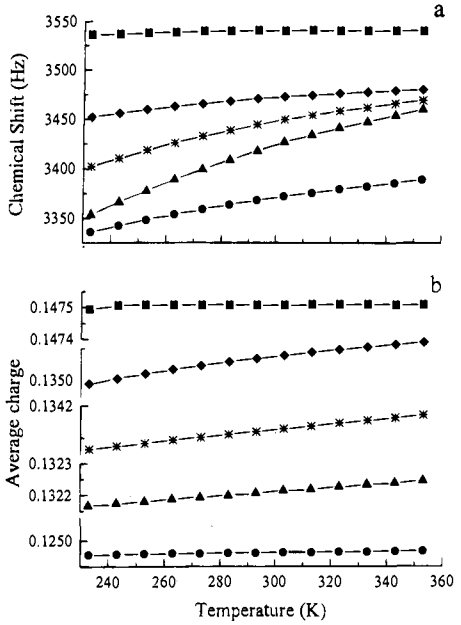


**Figure 11.** (a) Experimental temperature dependence of $^1$H NMR resonances for TBSxT. (b) Temperature dependence of aromatic proton charges, calculated as described in the text. For both a and b: (■) $H_a$, (●) $H_b$, (▲) $H_c$, (*) $H_d$, (♦) $H_e$.

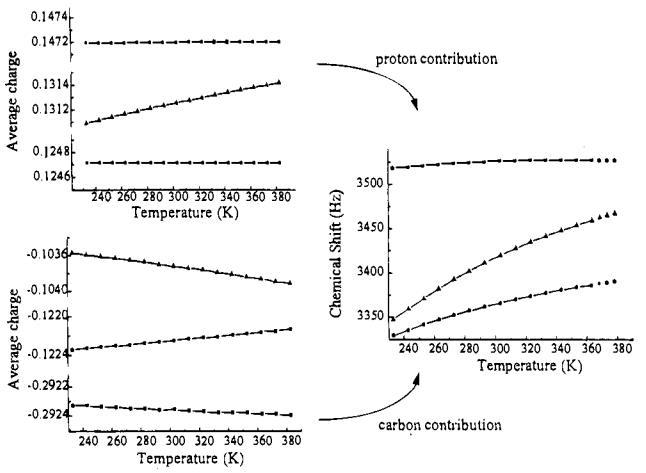


**Figure 12.** Calculated temperature-dependent proton charges (top, left) and aromatic carbon charges (bottom, left) for DBTT, compared to experimental $^1$H NMR chemical shift temperature-dependent data. The comparison is necessarily qualitative. See text for a discussion of this point. Symbol assignments are the same as in Figure 6.

coordinate is expected to be most limiting. We recognize that the magnitude of the chemical shift(s) in hertz is not calibrated, necessarily, with the temperature-dependent charge variation on each proton, due in part to the inherently qualitative nature of the molecular orbital calculations we used to estimate the charges. Registration of these two scales (charge and chemical shift) would be empirical even with the appropriate standards.[33,38] Thus our qualitative agreement between experiment and model is encouraging in and of itself. Previous models, relating electronic charge to $^1$H NMR chemical shift, have focused on the carbon atom to which the proton is bound. We observe that the charge on the proton is a dominant factor in determining the deshielding and thus the NMR chemical shift. The relationship between the charges on each proton and carbon and the proton chemical shift will be determined by proportionality constants that are different for each species.

Thus eq 1 can be modified to include these dependencies explicitly,

$$\Delta\delta_H = a_H\Delta q_H + a_C\Delta q_C \qquad (4)$$

where $a_H$ and $a_C$ are different. Consideration of either of these charges individually does not provide the optimum agreement, although it is clear from the experimental data that the dominant contribution to $\Delta\delta_H$ comes from $a_H\Delta q_H$. Consideration of $a_C\Delta q_C$ would lead to an improved correlation between experiment and model, as suggested by Figure 12. While we can calculate the terms $q_C$ and $q_H$, the determination of each coefficient $a$ is problematic because of the limited experimental information available. That is, we do not have sufficient experimental information to determine either $a_C$ or $a_H$ separately. Despite this limitation, we recognize that the trends presented in the experimental data are consistent with contributions from the electron densities of both the proton and carbon. Proton a of DBTT will exhibit relatively little temperature dependence because the charge density on the carbon to which it is attached is comparatively rotation independent. The temperature dependence of the proton b NMR resonance will increase in slope due to the inductive effect of the adjacent carbon, and proton c will exhibit a slight decrease in its temperature dependence. The comparisons between experimental NMR data and our calculated charge temperature dependencies are in excellent predictive agreement with the relationship between electronic charges and chemical shift indicated in eq 4. The agreement between the experimental data and our model also provides justification for our estimation of an isomerization barrier on the order of 8 kcal/mol for ground state thiophene oligomers, as calculated. A few words are in order at this point on the meaning(s) of the isomerization barriers we report in Figures 6–8. For DBTT, there is only one unique dihedral angle, and the barrier height of ~10 kcal/mol calculated for this isomerization is determined almost exclusively by steric constraints imposed by the *n*-butyl moieties at the 3′ and 4′ positions of the molecule. Our calculation did not take into account the ability of these aliphatic groups to move in such a way as to minimize steric hindrance to the ring rotation, and we thus believe that the calculated barrier is a slight overestimate of the actual experimental barrier. For the larger oligomers, DBPtT and TBSxT, the barriers we report in Figures 7 and 8 are averages of the isomerization barriers for the 2 (DBPtT) or 3 (TBSxT) dihedral angles involved. We recognize that the ~8 kcal/mol barrier is an overestimate for the DBPtT terminal ring because steric hindrance by the *n*-butyl groups will not play a role. For rotation of only the DBPtT terminal ring, we calculate an isomerization barrier of ~1 kcal/mol. The relatively poorer agreement between experiment and calculation for this oligomer (Figure 10) is therefore an expected result. For TBSxT, the rotation of each thiophene ring will be hindered to some extent by the presence of the *n*-butyl groups on an adjacent ring, and thus the average of the barriers will provide a reasonably accurate one-dimensional representation of the isomerization surface of this molecule. Because of the qualitative nature of the calculations, and the limitations intrinsic to our reduction of these complex, large amplitude molecular motions to a one-dimensional coordinate, we do not imply that 8 kcal/mol is an explicit upper or lower bound on the isomerization barrier energy for these molecules. We assert, however, that the experimental barriers must be close to those we calculate. If the barriers to ring rotation were much higher than 8 kcal/mol, the temperature dependence of the NMR resonances would be much weaker because the oligomers would remain in energetically favored conformations even at elevated temperatures, *i.e.* a small portion of the multidimensional isomerization surface would be sampled. Conversely, if the isomerization barrier were negligible com-

pared to $k_BT$, then the isomerization surface would be sampled uniformly for all temperatures and we would observe a temperature-independent $^1H$ NMR response. The correlation between the semiempirical calculations and the experimental NMR data also indicates that the electron density on the protons is at least as important as the charge on the carbons in determining the proton chemical shift for aromatic systems.

**Excited State Isomerization.** Dilute ($\sim 10^{-4}$ M) solutions of DBPtT and TBSxT in methanol, *n*-butanol, *n*-heptanol, and *n*-decanol were excited at 390 and 406 nm, respectively, and fluorescence was collected at the wavelengths indicated in Table 1. The lifetimes were observed by collecting fluorescence polarized at 54.7° with respect to the exciting electric field to eliminate any rotational diffusion contributions to the data. In a previous report, the lifetime of DBTT showed a linear dependence on viscosity, which can be understood in the context of the existence of an excited state rotamer that is coupled efficiently to the ground state surface. For this model, there is essentially ~90° of uncertainty in the interring dihedral angle at which efficient relaxation occurs. Many organic molecules exhibit a minimum energy in their $S_1$ isomerization surfaces at an inter-ring dihedral angle of 90°, because of the decoupling of the $\pi$ system (break in conjugation) at this dihedral angle.[43,44] Relaxation from this conformation is thought to be rapid, and the limiting rate in the relaxation of the excited electronic state in this model is therefore mediated by the time required to execute an activated isomerization along the $S_1$ surface. The other possibility is that there is no 90° conformer that relaxes efficiently, but rather, one conformer is significantly shorter lived than the other conformer. These two conformers are expected to differ by an inter-ring dihedral angle of ~180°. In other words, the ~*syn* conformer excited state lifetime is expected to be significantly different than that of the ~*anti* conformer. The obvious difference between these conformers is the extent to which S atoms on adjacent rings can interact. We speculate that such an interaction, enhanced in the ~*syn* conformer, would serve to decrease the excited state lifetime, although there is no direct data to support this speculation. Semiempirical calculations of the $S_1$ thiophene oligomers (not shown) predict isomerization surfaces that do not exhibit energetic minima at 90° dihedral angles, but rather indicate the presence of energetic maxima at 90°.

Regardless of the model used, the time required for an excited thiophene oligomer to relax is mediated by two barriers to the ring rotation: one intrinsic to the molecule and one imposed by the surrounding solvent medium. The extrinsic portion of the isomerization barrier, contributed by frictional interactions between the oligomer and the surrounding solvent, can be controlled by changing the solvent viscosity. In this model, a high viscosity solvent will impede the intramolecular ring rotation significantly, producing a comparatively long excited state lifetime.

For a low-viscosity solvent, where intramolecular motion is comparatively unhindered, the lifetime is expected to be shorter due to the greater rotational mobility of the rings. In order to estimate the intrinsic barrier to ring rotation for the thiophene oligomers, the viscosity dependence of the $S_1$ lifetime was extrapolated to zero viscosity. The experimental data for DBTT were regressed to a 123 ps zero-viscosity fluorescence lifetime. This lifetime can be interpreted in the context of an activated process,

(43) Rulliere, C. *Chem. Phys. Lett.* **1976**, *43*, 303.
(44) Awad, M. M.; McCarthy, P. K.; Blanchard, G. J. *J. Phys. Chem.* **1994**, *98*, 1454.

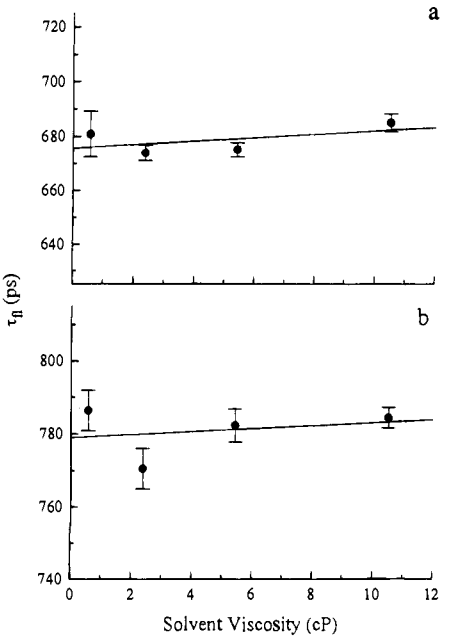


**Figure 13.** (a) Viscosity dependence of fluorescence lifetimes for DBPtT. (b) Viscosity dependence of fluorescence lifetimes for TBSxT.

$$k_{isom} = A \exp(-(E_{isom} + E_{vis})/k_BT) \quad (5)$$

using a preexponential factor of $10^{13}$, which is appropriate for the *n*-alcohols. From this time constant, $E_{isom}$ was determined to be 4.2 ± 0.4 kcal/mol, with the uncertainty in this value being determined by uncertainty in the value of *A*. For the longer thiophene oligomers DBPtT and TBSxT, we find that there is no discernible viscosity dependence, as shown in Figure 13. Despite the outward difference in the appearance of the DBPtT and TBSxT data compared to the data for DBTT, we believe that the same model applies because of the structural similarity of these molecules. We are confident in this assertion based on the similarity of the ground state barriers for all of these oligomers, as well as the qualitative similarities in their linear optical responses. If the intrinsic barrier to rotation is greater than the extrinsic isomerization barrier, due to solvent fractional forces, then little or no viscosity dependence will be observed. The lifetimes for DBPtT and TBSxT are 676 ± 4 and 779 ± 8 ps, from which rotational barriers of 5.1 ± 0.4 and 5.2 ± 0.4 kcal/mol were calculated. These barriers are approximately 1 kcal/mol higher than that of DBTT,[4] and we can rationalize this behavior in the context of a more delocalized $\pi$ system for the longer oligomers. We expect that the excited state of polythiophenes should be qualitatively similar to that of other conjugated polymers, such as polyaniline or poly(phenylenevinylene). For such polymers, the excited electronic state is expected to increase the bond order of the interring bond(s). The longer the oligomer, the more capable it will be of supporting a "quinoid-like" resonance structure,[9] and the larger will be the expected isomerization barrier. The experimental data and intuitive reasoning we describe above are consistent with semiempirical calculations of the excited thiophene oligomers, which indicate an $S_1$ barrier height of ~5 kcal/mol for both DBPtT and TBSxT.

## Conclusions

We have investigated the isomerization characteristics of several thiophene oligomers in order to understand the dependence of oligomer length on the intrinsic disorder in resulting polythiophenes. We find that the interring isomerization barrier

is ~8 kcal/mol for rotation in the $S_0$ state of all oligomers we have examined. This estimation is based on the temperature dependence of the $^1H$ NMR resonances for the aromatic protons and is not derived from a coalescence measurement.

For the $S_1$ DBPtT and TBSxT oligomers, we have determined isomerization barriers of 5.1 ± 0.4 and 5.2 ± 0.4 kcal/mol, respectively. These barrier heights are ~1 kcal/mol larger than that found for DBTT, and we rationalize this difference in the context of the longer oligomers being able to support a more quinoid-like excited electronic state. Our findings imply that the small barrier height values we have determined preclude the existence of corresponding long-term order in the polymers synthesized from these materials. The similarities of the isomerization barriers in these two states indicate that there is no significant basis for favoring a photopolymerization scheme over an electrochemical route. We speculate, based on these data, that the ground state inter-ring isomerization barriers for poly(thiphene)s are on the order of ~8 kcal/mol plus any additional frictional contribution associated with the motion of associated aliphatic moieties. Thus rotational defects in poly(thiophene)s do not likely contribute significantly to the material properties because any mesoscopic or macroscopic material response is averaged over a large number of rotations of each thiophene ring. If the ground state ring rotations in the polymer can be treated as an activated process, then the time constant for a ring rotation should be on the order of 60 ns. In this limit, extrinsic frictional effects in the solid state polymer will likely dominate the speed of ring rotation in these materials, but in any event such rotation will be effectively fast.

**Acknowledgment.** We thank the Michigan State University Center for Fundamental Materials Research for partial support of this work and Professor, M. D. Curtis for insightful suggestions on the DBTT work.

JA951291S